ARMY RESEARCH LABORATORY

Mechanical Response of Polycarbonate with Strength Model Fits

by Ajmer Dwivedi, Jermaine Bradley, and Daniel Casem

ARL-TR-5899 **February 2012**

NOTICES

Disclaimers

The findings in this report are not to be construed as an official Department of the Army position unless so designated by other authorized documents.

Citation of manufacturer's or trade names does not constitute an official endorsement or approval of the use thereof.

Destroy this report when it is no longer needed. Do not return it to the originator.

Army Research Laboratory
Aberdeen Proving Ground, MD 21005-5069

ARL-TR-5899 **February 2012**

Mechanical Response of Polycarbonate with Strength Model Fits

Ajmer Dwivedi and Jermaine Bradley
Dynamic Science, Inc.

Daniel Casem
Weapons and Materials Research Directorate, ARL

REPORT DOCUMENTATION PAGE	Form Approved OMB No. 0704-0188

1. REPORT DATE *(DD-MM-YYYY)*	2. REPORT TYPE	3. DATES COVERED (From - To)
February 2012	Final	October 2010–October 2011

4. TITLE AND SUBTITLE
Mechanical Response of Polycarbonate with Strength Model Fits

5a. CONTRACT NUMBER
W911QX-09-C-0057

5b. GRANT NUMBER

5c. PROGRAM ELEMENT NUMBER

6. AUTHOR(S)
Ajmer Dwivedi,* Jermaine Bradley*, and Daniel Casem

5d. PROJECT NUMBER

5e. TASK NUMBER

5f. WORK UNIT NUMBER

7. PERFORMING ORGANIZATION NAME(S) AND ADDRESS(ES)
U.S. Army Research Laboratory
ATTN: RDRL-WMP-B
Aberdeen Proving Ground, MD 21005-5069

8. PERFORMING ORGANIZATION REPORT NUMBER
ARL-TR-5899

9. SPONSORING/MONITORING AGENCY NAME(S) AND ADDRESS(ES)

10. SPONSOR/MONITOR'S ACRONYM(S)

11. SPONSOR/MONITOR'S REPORT NUMBER(S)

12. DISTRIBUTION/AVAILABILITY STATEMENT
Approved for public release; distribution is unlimited.

13. SUPPLEMENTARY NOTES
*Dynamic Science, Inc., 1003 Old Philadelphia Rd., Ste. 210, Aberdeen, MD 21001

14. ABSTRACT
Experiments were conducted on polycarbonate to investigate how the material responds mechanically at varying deformation rates and elevated temperatures. The data was then used to determine parameters for the Johnson-Cook strength model and the Zerilli-Armstrong polymer strength model. Quasi-static tests were conducted at strain rates between 0.005/s and 0.4/s using a servo-hydraulic load frame. Dynamic compression experiments were performed using the Split Hopkinson Pressure Bar and resulted in strain rates between 1750/s and 15,000/s. Pre-heated specimens were tested in both setups to determine the effects of thermal softening. The results indicate that the material response is rate sensitive with an enhanced hardening at rates greater than 10/s. Predictably, tests conducted at elevated temperatures cause a decrease in the apparent yield and flow stress. Model fits to the data are shown to provide a reasonable approximation of real world behavior.

15. SUBJECT TERMS
transparent materials, rate effect, temperature effect, polymer polycarbonate, polymer testing, kolsky bar, polymer modeling, plastic

16. SECURITY CLASSIFICATION OF:			17. LIMITATION OF ABSTRACT	18. NUMBER OF PAGES	19a. NAME OF RESPONSIBLE PERSON
a. REPORT	b. ABSTRACT	c. THIS PAGE			Ajmer Dwivedi
Unclassified	Unclassified	Unclassified	UU	32	19b. TELEPHONE NUMBER (*Include area code*) 410-306-0790

Standard Form 298 (Rev. 8/98)
Prescribed by ANSI Std. Z39.18

Contents

List of Figures

List of Tables

Preface

This report is the result of a collaborative effort between government and contractor personnel. Ajmer Dwivedi of Dynamic Science, Inc. (DSI) and Jermaine Bradley (DSI) conducted the experiments and performed data analysis. Daniel Casem was responsible for selecting appropriate constitutive models and accordingly designing experiments that would generate the necessary data.

Acknowledgments

The authors would like to thank Stephen Whittie (ORISE) and David Gray (RDRL-WMM-B) for their assistance setting up digital photography and operating servo hydraulic test platforms.

INTENTIONALLY LEFT BLANK.

1. Introduction

One of the most important applications for amorphous polymers is in transparent armor packages. Typically, these systems consist of alternating glass and transparent polymer layers. The glass serves to deform and fracture the threat while the polymer layer acts as a spall shield (*1*, *2*). Polycarbonate (PC) is a material that has high ductility and low density, making it a good candidate for use in these packages. PC is also being considered for several specialized applications because it has the potential to offer significant weight savings and better protection against relevant threats. To support ongoing research in these areas, experiments were conducted on PC to characterize its mechanical response.

The experiments performed as part of this study were used to determine material constants for constitutive models. These include uniaxial stress compression at both low and high rates as well as elevated temperatures. Low rate experiments (<1/s) were performed with a servo-hydraulic load frame and high rate tests (~10^3/s) with the Split Hopkinson Pressure Bar (SHPB) or Kolsky Bar technique. These experiments were supplemented with low rate tensile tests. Material constants were calculated for the Johnson Cook (JC) strength model and the Zerilli Armstrong (ZA) polymer constitutive model (*3*–*5*).

2. Material

The specimens used in this study were machined from a 12.7-mm thick Bayer MAKROLON General Purpose cast polycarbonate plate. Compression experiments performed on specimens taken from the thickness direction and two orthogonal directions revealed no evidence of anisotropy.

Table 1 lists the mechanical properties of the material. The densities of six specimens were measured using a water buoyancy method and the average value was found to be 1197.75 kg/m^3 with a standard deviation of 0.10 kg/m^3. Longitudinal and shear wave speeds have been reported by Millet and Bourne (*6*); assuming linear elastic behavior, elastic constants can be calculated. The wave speeds in the table are in agreement with the work of Carter and Marsh *(7)* who report longitudinal and shear wave speeds of 2.19 km/s and 0.89 km/s respectively.

Table 1. Material properties for PC. [a]Denotes value calculated by Millet and Bourne *(6).*

Density *(kg/m^3)*=	1197.75
[a]$C_{Longitudinal}$ *(km/s)*=	2.13
[a]C_{Shear} *(km/s)*=	0.88
Modulus of Elasticity *(GPa)*=	2.59
Shear Modulus*(GPa)*=	0.93
Lamé Constant *(GPa)*=	3.58
Bulk Modulus *(GPa)*=	4.20

3. Experimental Procedures

3.1 Low Rate Compression and Tension

Quasi static compression tests were conducted using an Instron model no. 1331 servo-hydraulic load frame. During the tests a 22.2 kN load cell measured the force applied to the specimen and a linear variable differential transformer (LVDT) measured the crosshead displacement.[*] Strain rates using this setup varied from 0.005/s up to 0.4/s. The specimens were cylindrical and had nominal dimensions of 5×5 mm (length×diameter). The PC samples were loaded between two tungsten carbide platens and the contact surfaces were lubricated with MoS_2 grease to reduce friction. To perform low rate tests at elevated temperatures an Instron SFL Temperature Control Chamber was used. Specimens were compressed at temperatures of 38 °C, 54 °C, and 71 °C. During temperature tests the platens and actuator arms were heated to the desired temperature before the specimen was positioned. Once in place, the sample was allowed to rest for 15 min before testing to allow the temperature to equilibrate.

Low rate tension experiments were completed using the same Instron model no. 1331 machine previously described. A dimensioned drawing of the tension specimen can be found in figure 1. To accommodate these specimens threaded collars were attached to actuator arms of the load frame.

[*] Machine compliance corrections were incorporated into all data analysis.

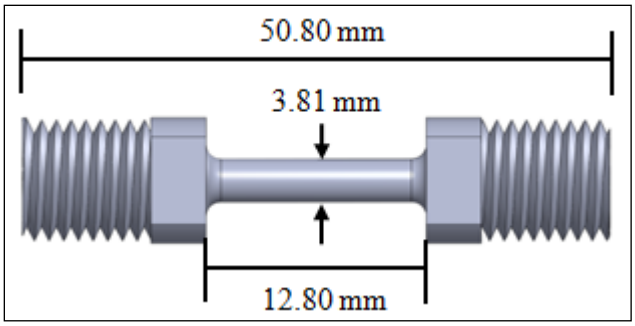

Figure 1. Dimensioned drawing of the tension specimen.

A Retiga 2000-R digital camera was used to record the deformation of the samples during tests and to provide a confirmation of measured strain.

3.2 High Rate Compression

High rate compression experiments were conducted using a SHPB (*8–10*). For strain rate experiments up to ~6500/s, 7075-T6 aluminum bars with diameters of 9.525 mm were used. In order achieve even higher rates (~15,000/s) specimens with a reduced gage length were tested using bars with a diameter of 4.76 mm. Cylindrical samples were tested in both setups and the associated dimensions were 5×5 mm and 2×2 mm respectively. These dimensions were chosen so that an aspect ratio of 1 would be maintained for all compression tests. Each bar was instrumented with two, diametrically opposed strain gages[†] to measure the elastic waves within the bars. As with the low rate tests, the contact surfaces of the PC samples were lubricated with MoS_2 grease. The data analysis for these experiments includes a correction for wave dispersion in the bars (*11–14*). During all dynamic tests adiabatic behavior is assumed.

Dynamic compression tests were also conducted at elevated initial temperatures to investigate the combined effects of strain rate hardening and thermal softening. An insulated chamber was constructed that enclosed the specimen and ~100 mm of both the incident and transmission bars. Hot air was then circulated throughout the chamber for ~20 min. Because soldering a thermocouple directly to the PC specimen was not possible, one was placed within 10 mm of the sample to measure ambient air temperature. It is assumed that given the soak time the air temperature at this location provides a reasonable approximation of specimen temperature.

[†] Two series of Vishay Micromeasurement strain gages were used: WK-06-250BF-10C and EA-13-062AQ-350.

4. Results

4.1 Low Rate and High Rate Compression at Room Temperature

Quasi static experiments were conducted at three strain rates: 0.005/s, 0.03/s, and 0.4/s. Figure 2 shows a representative stress strain curve at each rate. All three stress-strain curves in the figure display similar behaviors. First, stress increases nonlinearly up to a peak strain of ~0.08 mm/mm. It is assumed that this behavior is visco-elastic. Beyond this peak the flow stress begins to decrease as a result of strain softening. At a strain of 0.35 mm/mm, the flow stress begins to increase again due to strain hardening. These behaviors occur because of molecular chain rotations and translations and have been discussed in detail by Mehta and Prakash (*15*). This data suggests that the yield stress and to a lesser extent the elastic modulus (as indicated by the assumed elastic loading) are positively correlated to strain rate. Specimens were inspected at the conclusion of each test and no evidence of failure could be found. The results presented here are in agreement with the work of previous authors (*16–18*).

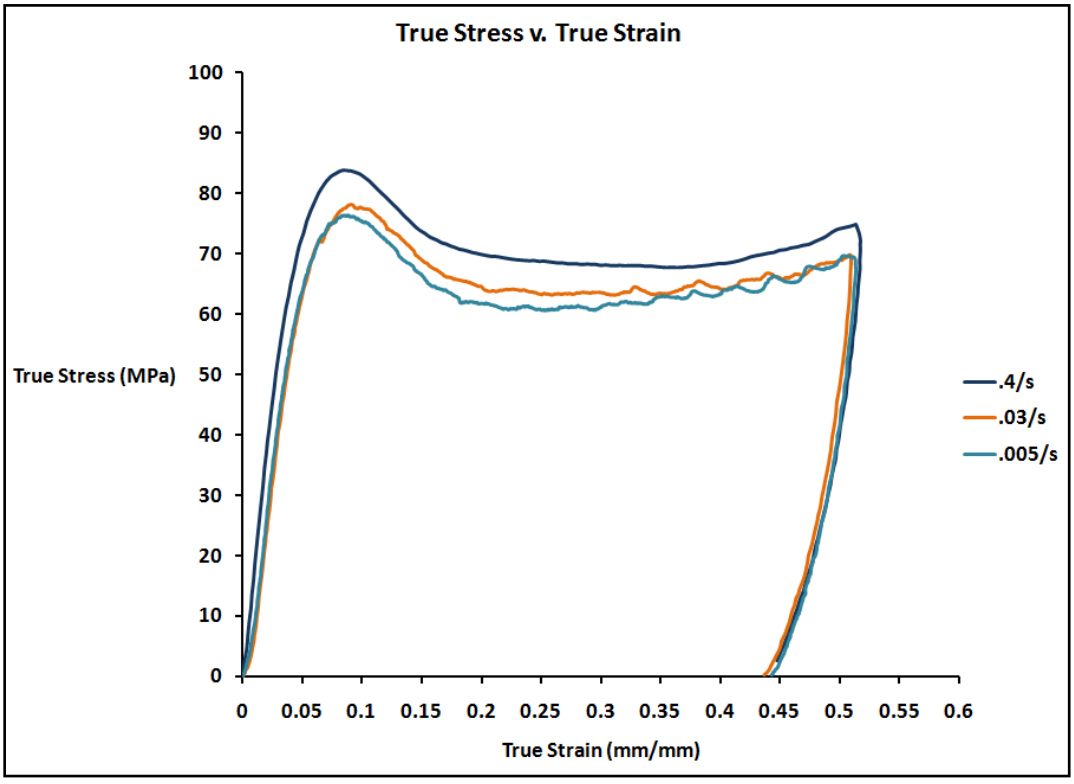

Figure 2. Representative stress – strain curves from low rate experiments.

SHPB compression tests were done at four different rates and figure 3 shows representative results for the tests. The same three behaviors noted in the low rate experiments are found here. The test conducted at 1750/s does not show evidence of strain hardening, but this is because the

specimen was only loaded to a strain of ~0.3 mm/mm. Also, the stress-strain curves did not return to zero stress because only a portion of the specimen unloading was recorded. Recovered specimens were visually inspected and there was no evidence of fracture. At some point between quasi-static and dynamic conditions, the strain rate effect on the apparent yield stress becomes decidedly more dramatic. This phenomenon occurs due to the activation of a secondary molecular process at high strain rates (*19–20*). Consequently, the polymer chains become stiffer and higher stresses are achieved.

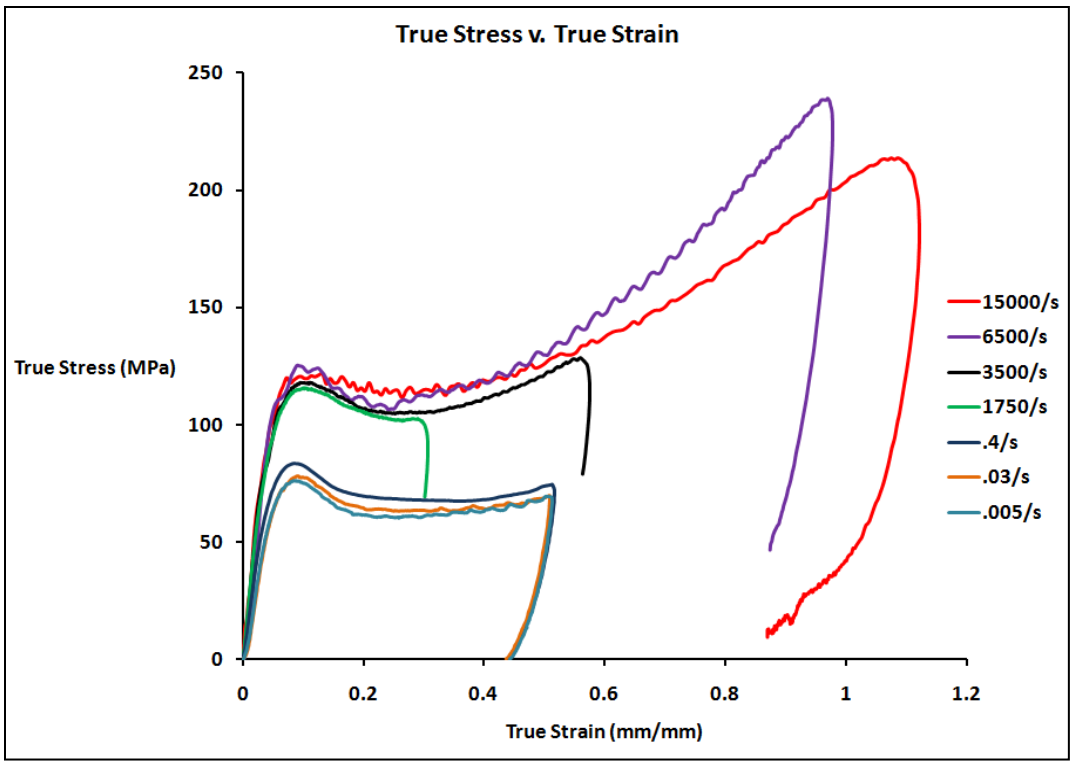

Figure 3. Representative stress – strain curves from SHPB compression tests.

In figure 4 the observed yield stress of PC is plotted as a function of the strain rate to determine an approximate activation strain rate for the secondary process. Logarithmic trendlines were fitted to the experimental data and extrapolated. The intersection of the extrapolated lines provides a rough estimate of where the transition to the more pronounced rate effect occurs. Based on the data the threshold strain rate is ~10/s, but others have reported it closer to 100/s (*20*). Additionally, it appears that beyond 3500/s, higher strain rates begin to have a diminishing effect on the yield behavior.

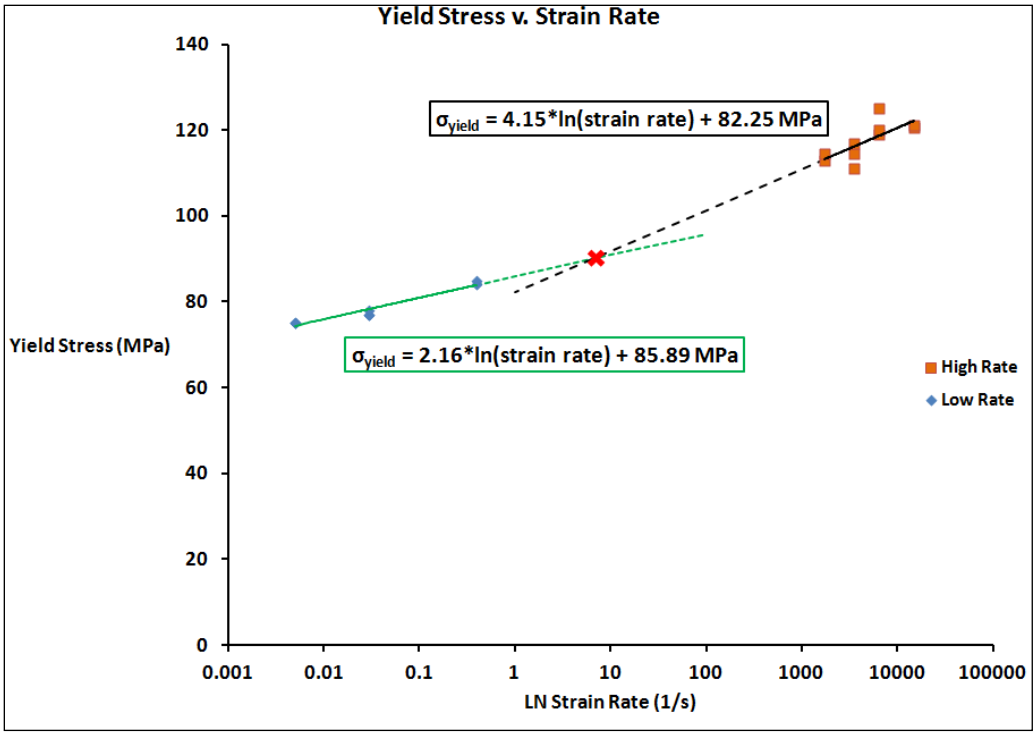

Figure 4. Yield stress as a function of strain rate. Extrapolation of linear fits (dotted) suggest a transition to enhanced hardening at ~10/s.

4.2 Compression at Elevated Temperatures

Select results from elevated temperature tests are shown in figure 5. Predictably, higher temperatures result in decreased yield and flow stresses. Figure 6 shows the yield stress from all the experiments as a function of temperature. Low temperature tests (i.e., below room temperature) were not conducted as part of this program, but several researchers have performed such experiments (*16, 18, 19*). They found that lower temperatures have the reverse effect, i.e., increased yield and flow stresses. Similar to the high rate tests, these increases are attributed to the restriction of secondary molecular motions.

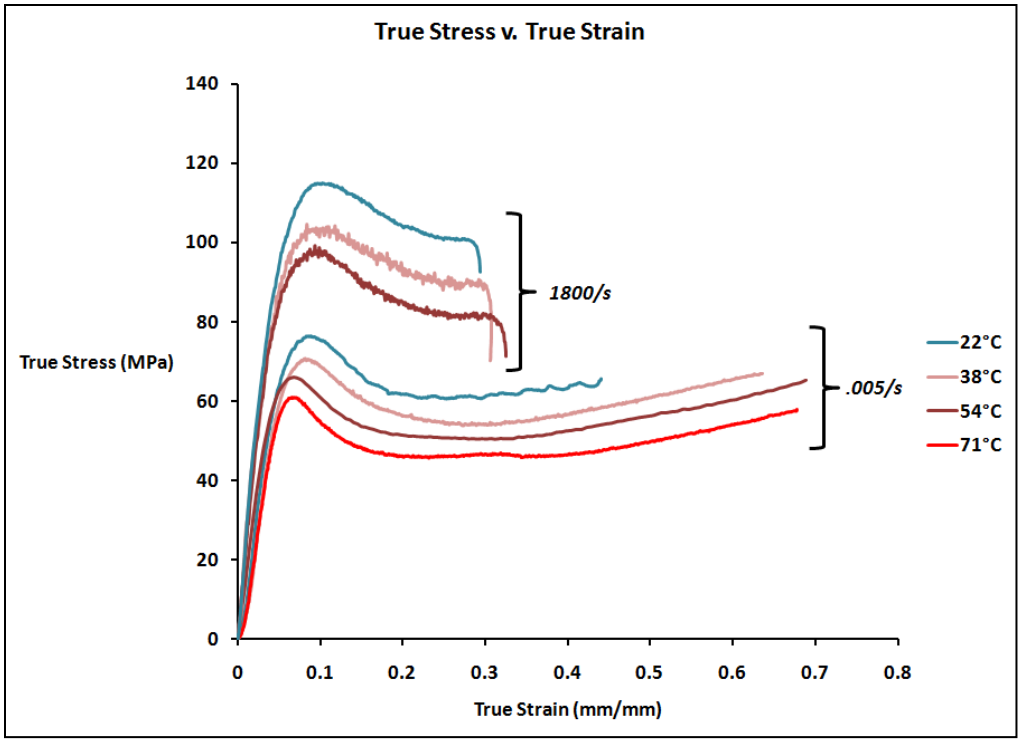

Figure 5. Results from compression tests at elevated temperatures.

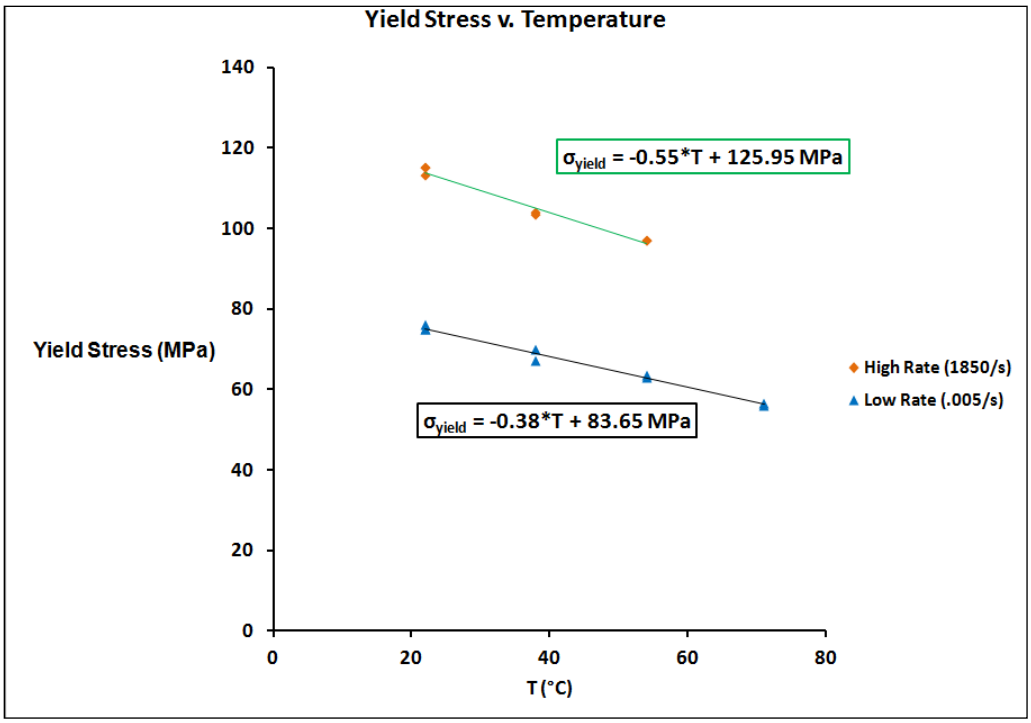

Figure 6. Yield stress as a function of temperature.

4.3 Low and High Rate Tension

Figure 7 shows engineering stress-strain curves from low rate tensile tests using the dog bone specimen shown in figure 1. A singular compression test is included in the figure for comparison. As in compression, the tensile data shows regions of visco-elastic loading, softening, and hardening. An interesting observation from the experiments was the tendency of the neck to propagate along the gage length as shown in figure 8. The movement of the neck along the length of the specimen corresponds to the relatively flat portion of the stress strain curve between 0.1 mm/mm and 0.4 mm/mm. Once propagation has finished the flow stress begins to increase due to hardening. A detailed discussion of this behavior has been presented by Wu and Van Der Giessen (*21*).

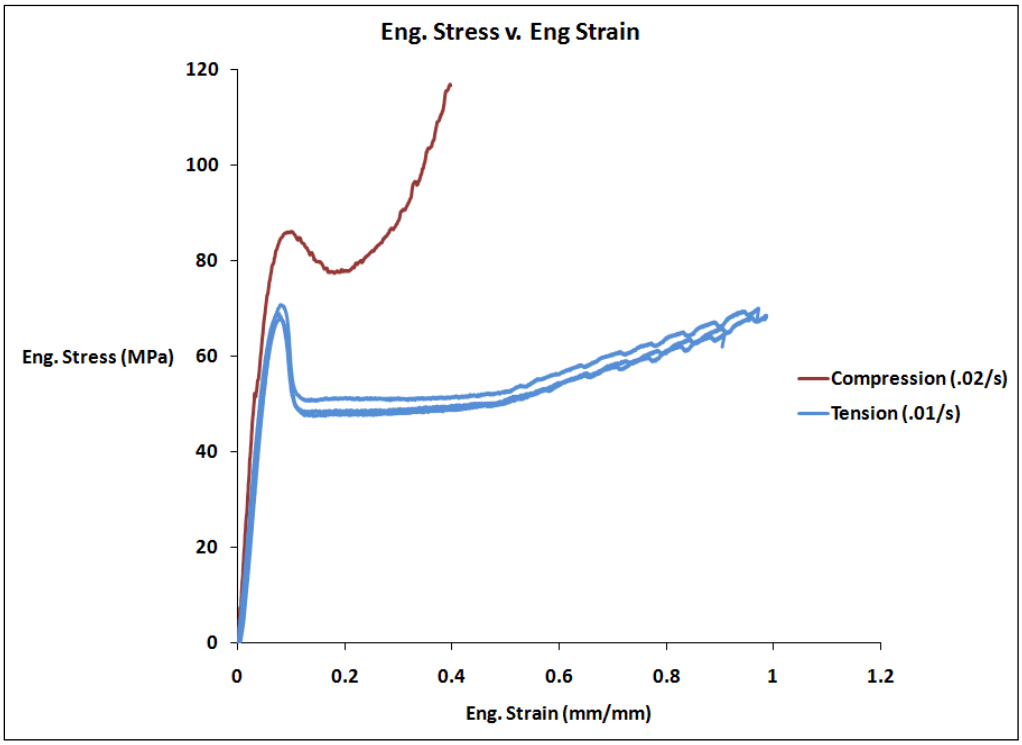

Figure 7. Results from low rate tension experiments.

Dynamic tension experiments were not performed as part of this study, but the high rate tensile response of PC has been documented. Cao et al. (*22*) conducted high rate tension experiments and found that tensile yield and flow stresses are positively correlated to strain rate. They report that for tests at rates between 370/s and 1700/s yield tends to occur at roughly 10% engineering strain at a stress of 100 MPa. Sarva and Boyce (*23*) also performed high rate tension experiments on PC. They were able to initiate two necks in straight gage specimens by altering the diameter of specimens while keeping the gage length constant. Additionally, they report that the formation of necks depends on the loading velocity and method used to grip the specimen. Finally, Sarva and Boyce successfully simulated the results from their experiments using the ABAQUS finite element code.

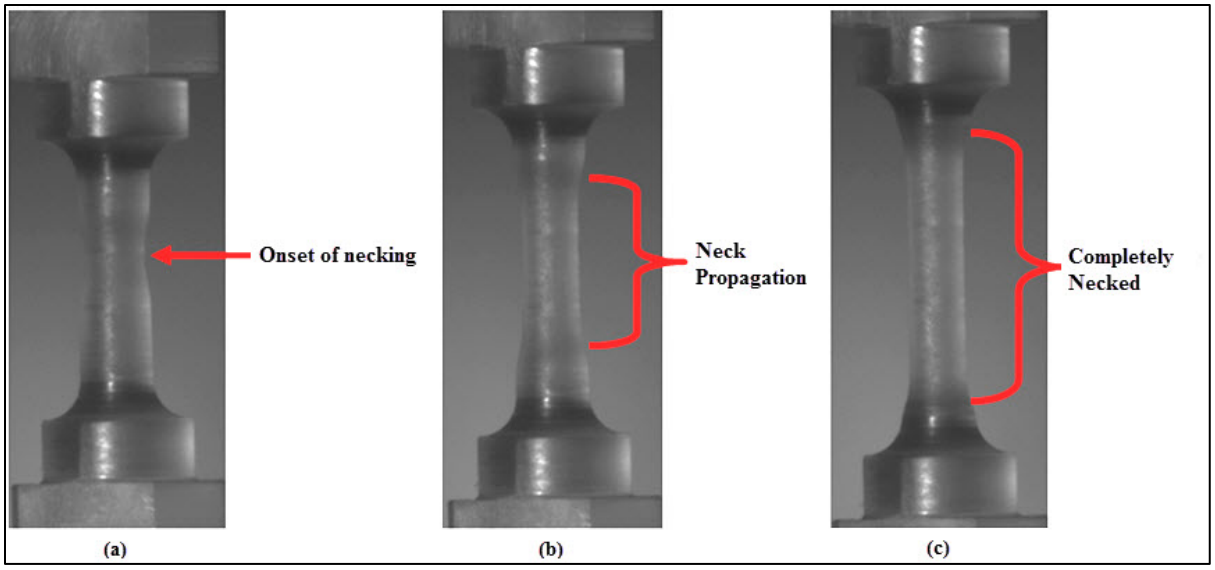

Figure 8. Neck propagation in straight tension specimens.

5. Constitutive Modeling

The experimental data was fit to the JC and ZA (polymer) constitutive equations. The JC equation is written as:

$$\sigma = \left(A + B{\varepsilon_p}^n\right)\left(1 + C\ln\frac{\dot{\varepsilon}}{\dot{\varepsilon}_0}\right)\left(1 - {T^*}^m\right) \quad (1)$$

where T* is the homologous temperature:

$$T^* = \frac{T - T_R}{T_m - T_R} \quad (2)$$

In the equation A, B, C, m, and n are all constants related to the material. T is the material temperature and T_R is a reference temperature, which in the present case is equivalent to room temperature. T_m is usually the melting temperature; here it is used as free-parameter to improve the quality of the fit. $\dot{\epsilon}$ is the strain rate and $\dot{\varepsilon}_o$ is the reference strain rate for which 1/s was used. This form of the JC constitutive model is readily available in most hydrocodes and for that reason it is often chosen to model material behavior.

To determine the material constants a series of least square fits to the experimental data are required. During this process, only the compression data is used. Assuming T = T_R = 295 K and $\varepsilon_p \approx 0$ values for A and C can be estimated from a logarithmic fit to the data in figure 4. Estimates of m and T_m can be obtained from a linear fit to the temperature data in figure 6. In this case a fit to the low rate data was used because a wider range of temperatures were available. As such it was assumed that $\dot{\epsilon}$=0.005/s and again that $\varepsilon_p \approx 0$. The remaining terms B and n can be

fit to the stress-strain curves in figure 3 assuming isothermal behavior at low rates (0.005/s–0.4/s) and adiabatic conditions at high rates (>0.4/s). For the adiabatic curves the specific heat capacity, Cv, was taken to be 1.3 KJ/kg-K. The ratio of plastic work converted to heat, β, was assumed to be 0.5 based on the work of Li and Lambros (*24*). Because the majority of the constants were estimated from yield data it is necessary to adjust each one to that value that best represents the experimental data.

Table 2 lists the JC parameters and figure 9 shows JC stress strain-curves compared to the experimental data. The JC constitutive equation was not intended to capture the softening that occurs after specimen yield and as such it does not represent the low rate (isothermal) data well. However, at high higher rates where adiabatic conditions are assumed the equation provides a reasonable approximation of the experimental data. This is because the introduction of thermal softening into the equation diminishes the strain hardening effects resulting in a better approximation of the constitutive behavior. Note that while activation of thermal softening in this equation provides a better approximation of the data, this is not the correct real world mechanism.

Table 2. JC parameters.

A=	80	*MPa*
B=	75	*MPa*
C=	0.052001	—
m=	0.548	—
n=	2	—
$\mathbf{T_{melt}}$=	562	*K*
β=	0.5	—
ρ=	1220	kg/m^3
$\mathbf{C_v}$=	1.3	*KJ/(kg K)*

The experimental data was also fit to a simplified form of the ZA polymer constitutive model that assumes no pressure dependence. While it is known that PC has some pressure dependence there is not enough available data to fit that aspect of the model. To estimate parameters for the simplified model the method outlined by Casem (*25*) was followed. Table 3 lists the constants for the ZA polymer constitutive model and figure 10 compares the ZA stress-strain curves to the experimental data. The model reasonably captures the material behavior, but significant variation persists despite the additional parameters. It was possible to adjust the constants so that they provided a very accurate representation for either the assumed isothermal or adiabatic conditions, but not both. The inability of both models to represent material behavior over the entire range of strain rates occurs because there is no mechanism in the equations to account for the transition to enhanced rate hardening as a result of the secondary molecular process.

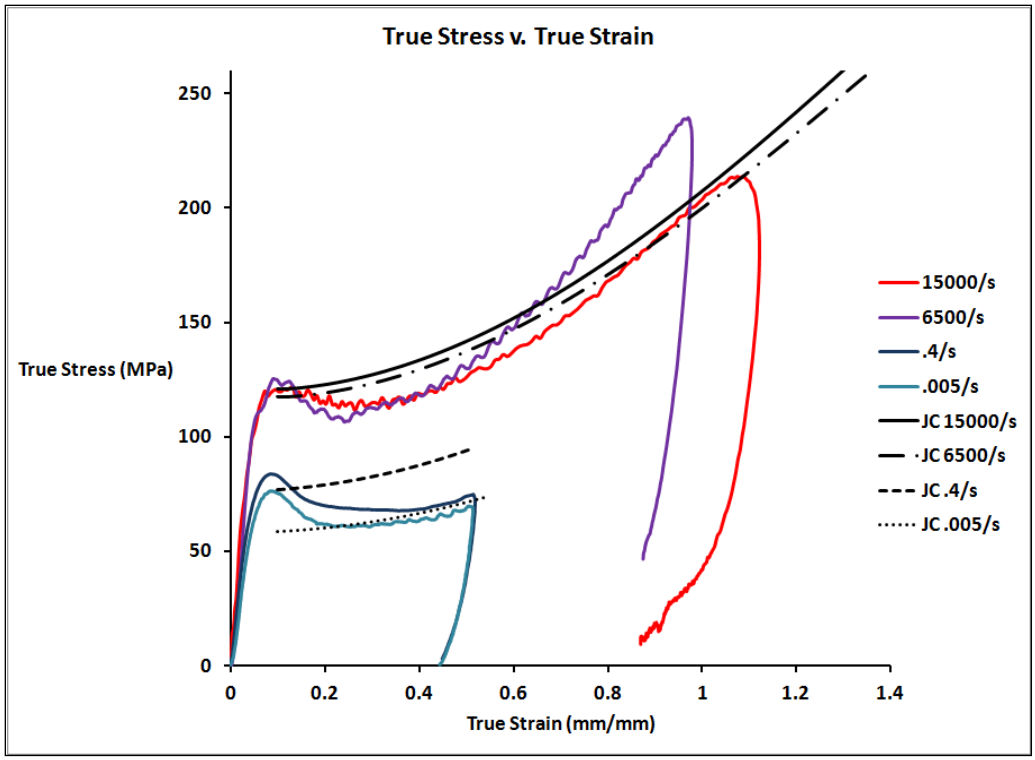

Figure 9. Comparison of JC calculations to experimental data.

Table 3. ZA model parameters.

$\mathbf{B_o}$=	0.006715948	*1/K*
$\mathbf{B_1}$=	0.00009503	*1/K*
$\mathbf{B_{pa}}$=	550	*MPa*
$\mathbf{B_{opa}}$=	48	*MPa*
$\boldsymbol{\omega_a}$=	-8	—
$\boldsymbol{\omega_b}$=	-0.01	—
$\boldsymbol{\beta}$=	0.5	—
$\boldsymbol{\alpha_{0=}}$	0.00655	*1/K*
$\boldsymbol{\alpha_{1=}}$	0.00004	*1/K*
ρ=	1220	kg/m^3
$\mathbf{C_v}$=	1.3	*KJ/(kg K)*

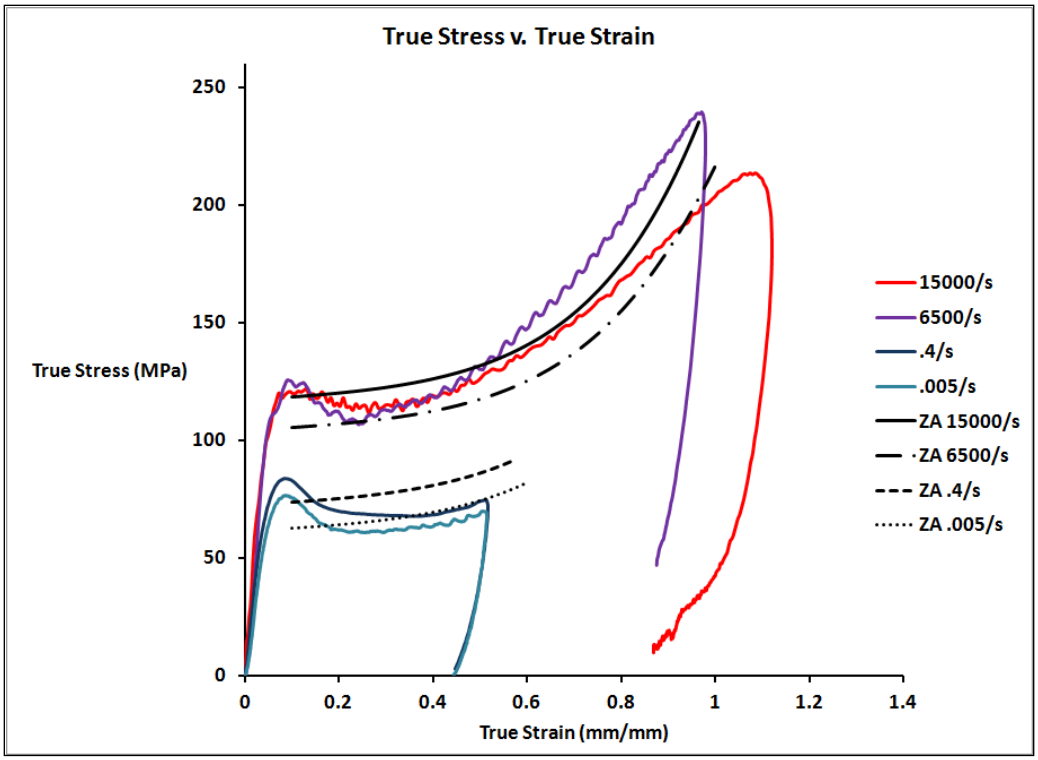

Figure 10. Comparison of ZA calculations to experimental data.

6. Discussion and Conclusion

A series of mechanical tests were conducted on polycarbonate to characterize its mechanical response. These included experiments in tension and compression and covered a strain-rate range of 0.001/s to 15k/s and a temperature range from 295 to 343 K. It was shown that strain rate and temperature are important factors that influence the material behavior. Data from the experiments were used to calculate parameters for the JC strength model and a simplified ZA polymer strength model. Both models were able to capture the basic features of the mechanical response and should be suitable for certain classes of impact problems.

Some significant drawbacks of the work exist. First and foremost is the absence of high-pressure data. The yield behavior of polycarbonate has been shown to be pressure dependent. This has been established from plate impact experiments, e.g., Millet and Bourne (*6*), who found that the shear strength of the material increases with pressure under uniaxial strain shock loadings. Limited work has been performed with the pressure shear plate impact method (PSPI) (*26–28*). Mehta and Prakash (*15*) have performed PSPI experiments on PC and found that a pressure of 1 GPa and strain rate of 400,000/s result in a significant increase in the yield (0.1 GPa) and flow

stress of the material. Furthermore, the authors reported that the material does not undergo any strain softening under these conditions.

In addition to the added component of pressure, these experiments have the further benefit of increased strain-rates (beyond 15 k/s). The higher rate data are beneficial for certain classes of ballistic problems, and is another shortcoming of the current work. Other methods to achieve high rate that would be appropriate for this material are miniature Kolsky bar methods, for example Casem et al. (*29*) have designed a miniaturized SHPB that allows experiments to be conducted at strain rates in excess of 150,000/s. Triaxial stress experiments with both servo-hydraulic and SHPB methods can also be employed to study the effects of pressure over a range of strain-rates.

In future work it is suggested that a more thorough constitutive model, such as the one presented by Mulliken and Boyce (*30*), be used to represent the data. Finally, experiments should be conducted to describe the fracture behavior of polycarbonate in a ballistic environment. Although more appropriate for metals, the JC fracture model could offer a place to start.

7. References

1. Patel, P. J.; Hsieh, A. J.; Gilde, G. A. Improved Low-Cost Multi-Hit Transparent Armor. *25th Army Science Conference*. 2006, Orlando, FL.

2. Hsieh, A. J.; DeSchepper, D.; Moy, P.; Dehmer, P. G.; Song, J. W. *The Effects of PMMA on Ballistic Impact Performance of Hybrid Hard/Ductile All-Plastic-and Glass-Plastic-Based Composites*; ARL-TR-3155; U.S. Army Research Laboratory: Aberdeen Proving Ground, MD, February 2004.

3. Johnson, G. R.; Cook, W. H. A Constitutive Model and Data for Metals Subjected to Large Strains, High Strain Rates, and High Temperatures. *Proceedings of the Seventh International Symposium on Ballistics*. The Hague (Netherlands), 1983, 541–547.

4. Zerilli, F.; Armstrong, R. A Constitutive Model Equation for the Dynamic Deformation Behavior of Polymers. *J. Material Sci.* **2007**, *42* (12), 4562–4574.

5. Zerilli, F.; Armstrong, R. Thermal Activation Based Constitutive Equations for Polymers. *J. Phys. IV France* **2007**, 10, Pr9. 3-8.

6. Millet, J. C.; Bourne, N. K. Shock and Release of Polycarbonate Under One-Dimensional Strain. *J. Material Sci.* **2006**, *41*, 1683–1690.

7. Carter, W. J.; Marsh S. P. *Hugoniot Equation of State of Polymers*; LA-12006-MS; Los Alamos National Laboratory: Los Alamos, NM, July 1995.

8. Follansbee, P. S. The Hopkinson Bar. In *Mechanical Testing, Metals Handbook*, 9th ed.; American Society for Metals: Metals Park, OH. 1985, Vol. 8, 198–217.

9. Meyers, M. A. Dynamic Behavior of Materials, John Wiley & Sons, Inc., New York, 1994.

10. Chen, W.; Song, B. Split Hopkinson (Kolsky) Bar, Springer LLC, 2011.

11. Gorham, D. A. A Numerical Method for the Correction of Dispersion in Pressure Bar Signals. *J. Phys. E.: Sci. Instrum.* **1983**, *16*, 477–479.

12. Folansbee, P. S.; Franz, C. Wave Propagation in the Split-Hopkinson Pressure Bar. *J. Eng. Mat. Tech.*, **1983**, *105*, 61.

13. Gong, J. C.; Malvern, L. E.; Jenkins, D. A. Dispersion Investigation in the Split-Hopkinson Pressure Bar. *J. Eng. Mat. Tech.* **1990,** *112*, 309–314.

14. Bancroft, D. The Velocity of Longitudinal Waves in Cylindrical Bars. *Phys. Rev.* **1941**, *59*, 588–593.

15. Mehta, N.; Prakash, V. Uniaxial Compression and Combined Compression-and-Shear Response of Amorphous Polycarbonate at High Loading Rates. *Proceedings of the SEM Annual Conference*, Albuquerque, New Mexico, 2009.

16. Blumenthal, W. R.; Cady, C. M.; Lopez, M. F.; Gray, G. T.; Idar, D. J. Influence of Temperature and Strain Rate on the Compressive Behavior of PMMA and Polycarbonate Polymers. *12th APS Topical Conference on Shock Compression of Condensed Matter*. Atlanta, Georgia, 2001.

17. Moy, P.; Weerasooriya, T.; Hsieh, A.; Chen, W. Strain Rate Response of a Polycarbonate Under Uniaxial Compression. *Proceedings of the SEM Annual Conference on Experimental Mechanics*, Charlotte, NC, June 2003.

18. Siviour, S. R.; Walley, S. M.; Proud, W. G.; Field, J. E. The High Rate Compressive Behavior of Polycarbonate and Polyvinylidene Diflouride. *J. Polymer.* **2005**, *46*, 12546–12555.

19. Richeton, J.; Ahzi, S.; Vecchio, K. S.; Jiang, F. C.; Adharapurapu, R. R. Influence of Temperature and Strain Rate on the Mechanical Behavior of Three Amorphous Polymers: Characterization and Modeling of the Compressive Yield Stress. *International Journal of Solids and Structures.* **2006**, *43*, 2318–2335.

20. Mulliken, A. D.; Boyce, M. C. Low to High Strain Rate Deformation of Amorphous Polymers. *Proceedings of the SEM Annual Conference on Experimental Mechanics*, Costa Mesa, CA, June 2004.

21. Wu, P. D.; Van Der Giessen, E. On Neck Propagation in Amorphous Glassy Polymers Under Plane Strain Tension. *International Journal of Plasticity* **1995**, *11* (3), 211–235.

22. Cao, K.; Xinzhong, M.; Baoshan, Z.; Wang, Y.; Wang, Yu. Tensile Behavior of Polycarbonate Over a Wide Range Strain Rates. *Material Science and Engineering (A)* **2010**, *527*, 4056–4061.

23. Sarva, S. S.; Boyce, M. C. Mechanics of Polycarbonate During High-Rate Tension. *Journal of Mechanics of Materials and Structures* **2007**, *2* (10), 1853–1880.

24. Li, Z.; Lambros, J. Strain Rate Effects on the Thermomechanical Behavior of Polymers. *International Journal of Solids and Structures* **2001**, *38*, 3549–3562.

25. Casem, D. T. *Mechanical Response of an Al-PTFE Composite to Uniaxial Compression Over a Range of Strain Rates and Temperatures*; ARL-TR-4560; U.S. Army Research Laboratory: Aberdeen Proving Ground, MD, September 2008.

26. Abou-Sayed, A. S.; Clifton, R. J.; Hermann, L. The Oblique Plate Impact Experiment. *Experimental Mechanics* **1976**, *16*, 127–132.

27. Clifton, R. J.; Klopp, R. W. Pressure-Shear Plate Impact Testing, Metals Handbook, 8 (9), American Society for Metals, Metals Park, OH, p.230–239, 1985.

28. Kim, K. S.; Clifton, R. J.; Kumar, P. Combined Normal-Displacement and Transverse-Displacement Interferometer with an Application to Impact of y-cut Quartz. *J. App. Phys*. **1977**, *48* (10), 4132–4139.

29. Casem, D. T.; Grunschel, S. E.; Schuster, B. E. Normal and Transverse Displacement Interferometers Applied to Small Diameter Kolsky Bars. *Experimental Mechanics,* Accepted.

30. Mulliken, A. D.; Boyce, M. C. Mechanics of the Rate Dependent Elastic-plastic Deformation of Glassy Polymers from Low to High Strain Rates. *International Journal of Solids and Structures* **2006**, *43*, 1331–1356.

List of Symbols, Abbreviations, and Acronyms

DSI	Dynamic Science, Inc.
JC	Johnson Cook
LVDT	linear variable differential transformer
PC	Polycarbonate
PSPI	pressure shear plate impact
SHPB	Split Hopkinson Pressure Bar
ZA	Zerilli Armstrong

NO. OF
COPIES ORGANIZATION

1 (PDF only) DEFENSE TECHNICAL INFORMATION CTR
DTIC OCA
8725 JOHN J KINGMAN RD
STE 0944
FORT BELVOIR VA 22060-6218

1 DIRECTOR
US ARMY RESEARCH LAB
IMNE ALC HRR
2800 POWDER MILL RD
ADELPHI MD 20783-1197

1 DIRECTOR
US ARMY RESEARCH LAB
RDRL CIO LL
2800 POWDER MILL RD
ADELPHI MD 20783-1197

1 DIRECTOR
US ARMY RESEARCH LAB
RDRL CIO MT
2800 POWDER MILL RD
ADELPHI MD 20783-1197

1 DIRECTOR
US ARMY RESEARCH LAB
RDRL D
2800 POWDER MILL RD
ADELPHI MD 20783-1197

NO. OF
COPIES ORGANIZATION

7 SOUTHWEST RSCH INST
C ANDERSON
K DANNEMANN
S CHOCRON
A NICHOLLS
D WAGAR
J RIEGEL
J WALKER
6220 CULEBRA RD
SAN ANTONIO TX 78238

2 SOUTHWEST RSRCH INST
T HOLMQUIST
G JOHNSON
5353 WAYZATA BLVD STE 607
MINNEAPOLIS MN 55416

1 RDTA RS MS 263
F RICKERT
6501 E ELEVEN MILE RD
WARREN MI 48397

1 LOS ALAMOS NAT LAB
THEORETICAL DIVISION
B CLEMENTS
MS B221
LOS ALAMOS NM 87545

ABERDEEN PROVING GROUND

1 DIR USA EBCC
SCBRD RT
5183 BLACKHAWK RD
APG EA MD 21010-5424

1 CDR USA SBCCOM
AMSCB CII
5183 BLACKHAWK RD
APG EA MD 21010-5424

1 DIR USAMSAA
AMSRD AMS D
BLDG 392

1 CDR USATEC
STEAC LI LV
E SANDERSON
BLDG 400

1 CDR US ARMY EVALUATION CTR
TEAE SVB
M SIMON
4120 SUSQUEHANNA AVE
APG MD 21005-3013

NO. OF
COPIES ORGANIZATION

1 US ARMY RSRCH LAB
ATTN RDRL ROE M S MATHAUDHU
PO BOX 12211
RESEARCH TRIANGLE PARK NC
27709-2211

147 DIR USARL
RDRL SL
R COATES
P TANENBAUM
RDRL SLB
R BOWEN
RDRL SLB A
P KUSS
J PLOSKONKA
B WARD
RDRL SLB D
R GROTE
D LOWRY
J POLESNE
RDRL SLB E
A DIETRICH
D LYNCH
RDRL SLB S
E HUNT
RDRL SLB W
W BRUCHEY
G DIETRICH
N EBERIUS
P GILLICH
W MERMAGEN
L ROACH
RDRL VTA
J BORNSTEIN
RDRL VTU
M NIXON
S WILKERSON
RDRL WM
L BURTON
B FORCH
S KARNA
J MCCAULEY
P PLOSTINS
T ROSENBERGER
W WINNER
RDRL WML
J NEWILL
T VONG
M ZOLTOSKI
RDRL WML D
A HORST
RDRL WML E
R ANDERSON
RDRL WML F

NO. OF COPIES	ORGANIZATION
	D LYON
	RDRL WML G
	W DRYSDALE
	RDRL WML H
	T FARRAND
	E KENNEDY
	L MAGNESS
	D SCHEFFLER
	S SCHRAML
	B SORENSEN
	R SUMMERS
	RDRL WMM
	J BEATTY
	R DOWDING
	J ZABINSKI
	RDRL WMM A
	S GHIORSE
	J ADAMS
	M MAHER
	J WOLBERT
	RDRL WMM B
	T BOGETTI
	B CHEESEMAN
	R DOOLEY
	C FOUNTZOULAS
	G GAZONAS
	C RANDOW
	M VANLANDINGHAM
	C YEN
	M FOSTER
	P MOY
	S WHITTIE
	RDRL WMM C
	R JENSEN
	RDRL WMM D
	E CHIN
	K CHO
	W ROY
	R SQUILLACIOTI
	S WALSH
	RDRL WMM E
	J CAMPBELL
	P DEHMER
	G GILDE
	T JESSEN
	J LASALVIA
	P PATEL
	J SANDS
	J SINGH
	RDRL WMM F
	R CARTER
	J CHINELLA
	K DOHERTY
	H MAUPIN

NO. OF COPIES	ORGANIZATION
	L KECSKES
	J MONTGOMERY
	D SNOHA
	RDRL WMP
	P BAKER
	B BURNS
	S SCHOENFELD
	RDRL WMP A
	C HUMMER
	B RINGERS
	RDRL WMP B
	A DWIVEDI (2 CPS)
	A GUNNARSSON
	C HOPPEL
	Y HUANG
	B SANBORN
	S SATAPATHY
	M SCHEIDLER
	T WEERASOORIYA
	RDRL WMP C
	R BECKER
	S BILYK
	T BJERKE
	J BRADLEY (2 HC)
	D CASEM
	J CLAYTON
	M GREENFIELD
	D DANDEKAR
	K KIMSEY
	B LEAVY
	C MEREDITH
	M RAFTENBERG
	S SEGLETES
	W WALTERS
	RDRL WMP D
	R DONEY
	T HAVEL
	S HUG
	M KEELE
	D KLEPONIS
	H MEYER
	R MUDD
	D PETTY
	J RUNYEON
	B SCOTT
	B VONK
	C WILLIAMS

NO. OF
COPIES ORGANIZATION

RDRL WMP E
S BARTUS
M BURKINS
W GOOCH
D HACKBARTH
E HORWATH
T JONES
D LITTLE
B LOVE
D SHOWALTER
RDRL WMM G
J LENHART
A HSIEH
RDRL WMP F
R BITTING
E FIORAVANTE
D FOX
A FRYDMAN
N GNIAZDOWSKI
R GUPTA
X HUANG
RDRL WMP G
R BANTON
N ELDREDGE
S KUKUCK

INTENTIONALLY LEFT BLANK.